Chemical Engineering Journal 108 (2005) 193–202

Chemical Engineering Journal

www.elsevier.com/locate/cej

Characterizing particle clustering behavior by PDPA measurement for dilute gas–solid flow

Xinhua Liu [a,b], Shiqiu Gao [a,*], Jinghai Li [a]

[a] *Multi-phase Reaction Laboratory, Institute of Process Engineering, CAS, Beijing 100080, PR China*
[b] *Graduate School of the Chinese Academy of Sciences, Beijing 100864, PR China*

Received 15 June 2004; received in revised form 18 January 2005; accepted 27 January 2005

Abstract

Based on particle velocity and size information measured by phase Doppler particle analyzer (PDPA), an algorithm to calculate particle cluster properties for dilute gas–solid flow was developed. The aggregate properties investigated in this study including voidage inside particle clusters, occurrence frequency, time fraction and particle cluster velocity show heterogeneous distributions in both axial and radial directions, although different properties differ from core to annulus region of the fluidized bed in their sensitivities to the variation of operating parameters. Experimental analysis shows that particle cluster properties are closely related to local time-averaged voidage and turbulent fluctuation of particles.

Keywords: Particle cluster; Dilute gas–solid flow; Phase Doppler particle analyzer; Fluidization

1. Introduction

Aggregation of particles is an important dynamic characteristic of gas–solid suspensions, and the characterization of particle clustering behavior is of great significance to the prediction of hydrodynamics of gas–solid flow by modeling. The formation of particle clusters has a critical effect on the spatial distributions of dynamic variables as well as the heat transfer coefficient in fluidized bed reactors [1]. The concept of particle clusters and their relevant empirical relationships have been incorporated in many mathematical models for circulating fluidized bed (CFB) dynamics [2,3].

Many properties including voidage inside particle clusters, occurrence frequency and time fraction are usually utilized to quantitatively characterize particle clustering behavior. For example, Tuzla et al. [4] studied the density, duration and time fraction of particle clusters in a downer fluidized bed by using a needle capacitance probe; Manyele et al. [5] characterized the frequency, time fraction, existence time, average solid concentration and vertical dimension of particle aggregates in a high-density CFB riser by using a fiber optic probe; Sharma et al. [6] investigated the parametric effects of particle size and gas velocity on the duration, frequency, time fraction and solid concentration of particle clusters in fast fluidized beds by using a needle capacitance probe. Harris et al. [7] correlated particle cluster properties in the near wall region with operating parameters of a vertical riser on the basis of published experimental data. Particle cluster dynamics in gas–solid suspensions has become a popular subject for investigation, but up to now, particle clustering behavior in dilute gas–solid flow has been paid little attention to, which might be due to a lower signal-to-noise ratio (SNR) of traditional probe measurement technique in dilute gas–solid suspensions. Although three different mechanisms – turbulent fluctuation of gas and solids [8], energy minimization [9] and particle-wake interactions [10] – have been proposed to explain the aggregation of particles, it remains a challenge for researchers to predict particle cluster characteristics via numerical modeling alone in order to further describe hydrodynamic behavior of gas–solid suspensions. Therefore, experimental study on particle clustering behavior in dilute gas–solid flow may help to understand the mechanism of

* Corresponding author. Tel.: +86 1 82627076.
E-mail address: sqgao@home.ipe.ac.cn (S. Gao).

1385-8947/$ – see front matter © 2005 Elsevier B.V. All rights reserved.
doi:10.1016/j.cej.2005.01.012

Nomenclature

A	effective flow area (m^2)
d	particle diameter (m)
d_{min}	minimal diameter detectable (m)
d_w	beam waist diameter (m)
D	effective diameter of probe volume (m)
f	frequency (Hz)
$f_{Doppler}$	frequency of Doppler bursts (Hz)
F	time fraction (%)
G_s	solids circulation rate (kg/m^2 s)
Gt	particle gate time (s)
H	elevation (m)
It	particle interval time (s)
K	optical constant (dimensionless)
Δl	space between two detectors (m)
L_D	Doppler burst length (m)
L_f	lens focal length (m)
L_{slit}	slit width (m)
m	mass (kg)
n	empirical constant (dimensionless)
N_{cl}	the number of clusters (dimensionless)
N_{min}	the required minimal number of fringes (dimensionless)
N_{probe}	the number of fringes inside the laser probe volume (dimensionless)
T	sampling time (s)
u	velocity (m/s)
U_g	superficial gas velocity (m/s)
y/Y	dimensionless distance (dimensionless)

Greek letters

α	half of the beam crossing angle (dimensionless)
δ	fringe spacing (m)
ε	voidage (dimensionless)
Φ	phase shift (dimensionless)
λ	wave length (m)
θ	collection angle (dimensionless)
ρ	density (kg/m^3)
σ_u	particle velocity standard deviation (m/s)

Subscripts

cl	particle cluster
g	gas
i, j, k	index of particle or particle cluster
p	particle
t	time-averaged
tr	transient

particle aggregation for dilute gas–solid suspensions comprehensively.

Compared with the probe method used generally under the condition of higher solid concentrations, phase Doppler particle analyzer (PDPA) measurement is a non-intrusive and powerful technique to study the aggregate properties of particles due to its capabilities in exploring both the micro and meso flow structures of dilute gas–solid suspensions [11]. Van den Moortel and Tadrist [12] have measured mean cluster axial lengths in a dilute gas–solid fluidized bed with the PDPA technique. This study will concentrate on the characterization of voidage inside particle clusters, occurrence frequency, time fraction and particle cluster velocity for dilute gas–solid flow by using PDPA.

2. Experimental

As shown in Fig. 1, experiments were conducted in a fluidized bed with a square cross-section of 0.1 m × 0.1 m and a height of 2.4 m. The measuring window on the bed wall

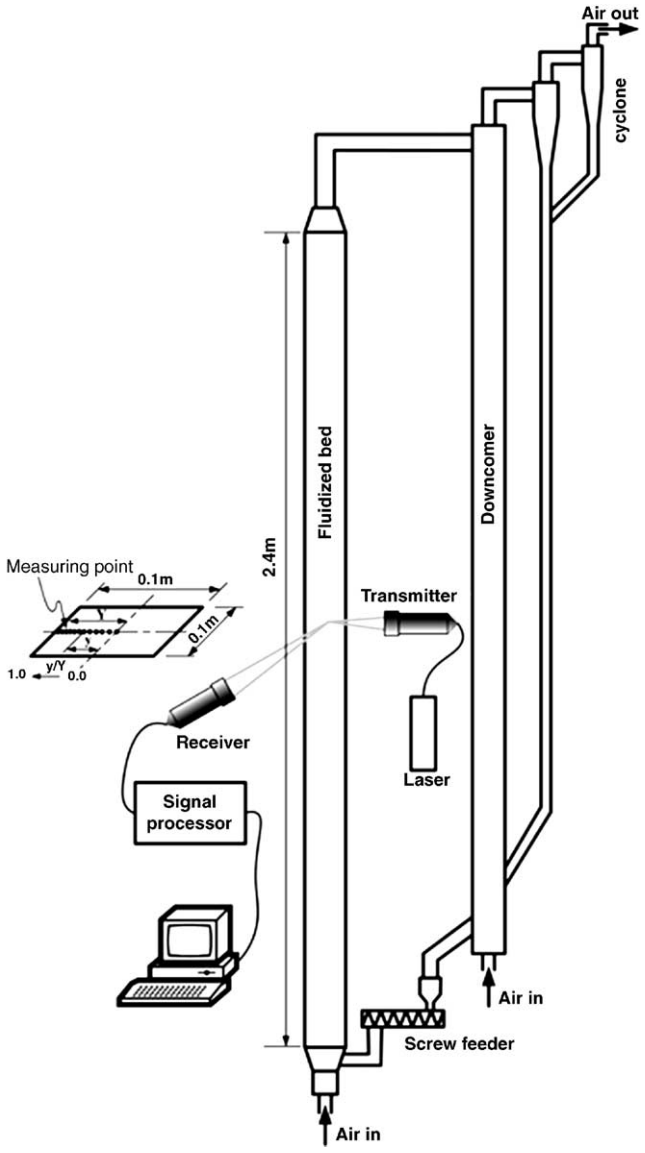

Fig. 1. Schematic diagram of experimental equipment and measuring point distribution.

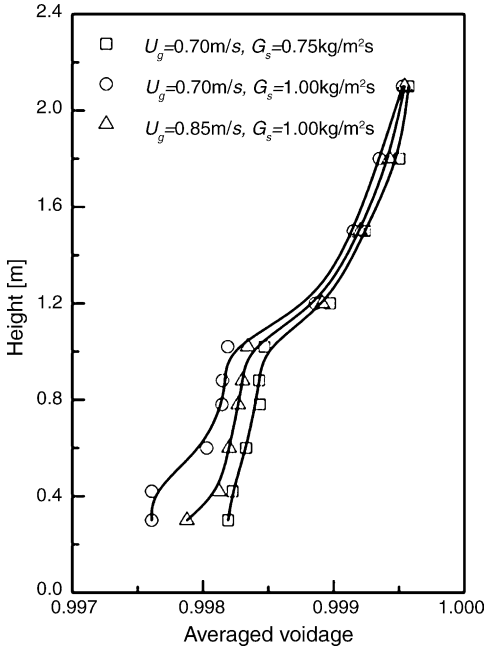

Fig. 2. Axial profile of averaged voidage.

is made of colorless plate glass with a thickness of 3 mm. Gas/solids separation was effected through a two-stage cyclone system and a bag filter. Solids circulation rate was measured by a butterfly valve fixed on a downcomer and controlled by a screw feeder at the bottom of the fluidized bed in order to make the fluidized bed operate in a dilute state. Measurements were taken on five different levels above the gas distributor (H = 0.71, 0.76, 0.81, 0.86 and 0.91 m) and at 12 different radial positions within a square test plane (y/Y = 0.00, 0.20, 0.36, 0.48, 0.60, 0.70, 0.80, 0.84, 0.88, 0.92, 0.96 and 0.98), where y/Y is the dimensionless distance from a measuring point to the central axis of the bed. The mean diameter and the density of glass beads as bed material are 53 μm and 2500 kg/m^3, respectively. The sphericity of glass beads is greater than 0.95.

All the experiments were carried out at superficial gas velocity U_g = 0.70–0.85 m/s and solids circulation rate G_s = 0.75–1.00 kg/m^2 s. According to Cai et al. [13], the calculated transition velocity from bubbling to turbulent fluidization is about 0.60 m/s. Therefore, the fluidized bed was operated in turbulent fluidization regime under the operating conditions. Neglecting wall friction and particle acceleration, the averaged voidage ($\bar{\varepsilon}$) in the fluidized bed can be calculated from pressure drop along elevation ($\Delta P/\Delta Z$) as follows:

$$\bar{\varepsilon} = 1 - \frac{\Delta P/\Delta Z}{(\rho_p - \rho_g)g}$$

As shown in Fig. 2, axial profile of the averaged voidage in the fluidized bed under different operating conditions shows that the test planes are located at a roughly constant section of averaged voidage (about 0.998), which indicates that the gas–solid flow in the fluidized bed is very dilute.

3. Measurement technique

A two-dimensional PDPA provided by Aerometric Ltd. was utilized in the experiments. According to the principle of PDPA measurement, Doppler bursts are produced when a particle passes through the ellipsoidal laser probe volume with a length of 2.833 mm and a diameter of 0.281 mm. The particle velocity u_p perpendicular to the test plane is proportional to the frequency of Doppler bursts:

$$u_p = \frac{\lambda}{2\sin\alpha} f_{Doppler} \quad (1)$$

The particle diameter d_p is correlated to the phase shift between two laser beams from two corresponding detectors at different position within the receiver:

$$d_p = \frac{L_f \delta\Phi}{2\pi\,\Delta l} K \quad (2)$$

The PDPA was placed at 30° off-axis from forward scattering direction to insure high light scattering intensities and to improve SNR. The relevant parameters of the PDPA system were summarized in Table 1.

In order to identify particle clusters from local transient solid concentration signals, Soong et al. [14] proposed reasonable criteria as follows: (1) the solid fraction in a cluster must be significantly above the time-averaged solid concentration at the same operating condition at the local position; (2) the perturbation in solid concentration due to occurrence of clusters must be greater than the random fluctuations in background solid fraction; (3) the concentration increase must be sensed for a sampling volume greater than the volume of a particle but smaller than the bed volume. These guidelines based on the capacitance probe measurement can also be extended to the PDPA measurement because similar time series information can be obtained from the two different measuring techniques. It is clear that the dimension of the laser probe volume in this work meets the third requirement of the criteria. The first two can also be met by setting a critical solid concentration for identifying particle clusters, so the premise to identify particle clusters from Doppler bursts is to obtain the time series of local transient solid concentrations at first. This problem has been solved by Sun et al. [15] by defining local transient solid concentration $1 - \varepsilon_{tr}$ as follows:

Table 1
Parameters of the PDPA system

Laser wavelength (nm)	514.5
Transmitting beam diameter (mm)	0.7
Beam waist diameter (μm)	281
Collection angle (°)	30
Lens focal length of transmitter (mm)	300
Beam separation (mm)	60
Lens focal length of receiver (mm)	500
Receiver aperture (μm)	100
Measurable velocity range (m/s)	−90 to 283
Measurable diameter range (μm)	0.5–90

$$1-\varepsilon_{\mathrm{tr}}=\sum_{i=1}^{k}\left(\frac{\pi}{6}d_{\mathrm{p}i}^{3}\right)/\sum_{i=1}^{k}[u_{\mathrm{p}i}A(d_{\mathrm{p}i})(\mathrm{Gt}_i+\mathrm{It}_i)] \tag{3}$$

where the numerator and denominator of the right-hand side represent the total and the swept volume of k particles, respectively. In general, if k in Eq. (3) equals the number of all particles detected in a sampling run, the calculated voidage represents local time-averaged voidage ε_{t}. While, if the particle series composed of k particles belongs to a particle cluster, the calculated $\varepsilon_{\mathrm{tr}}$ equals the voidage inside this particle cluster. Effective flow area $A(d_{\mathrm{p}i})$ of a particle was determined in detail by Liu et al. [11]:

$$A(d_{\mathrm{p}i})\approx D(d_{\mathrm{p}i})\frac{L_{\mathrm{slit}}}{\sin\theta} \tag{4}$$

where the effective diameter of the laser probe volume $D(d_{\mathrm{p}i})$ was defined by Saffman [16] based on the concept of the Doppler burst length:

$$D(d_{\mathrm{p}i})=\frac{\sqrt{6}d_{\mathrm{w}}}{2}\left[\frac{L_{\mathrm{D}}^{2}(d_{\mathrm{p}i})\cos^{2}\alpha}{d_{\mathrm{w}}^{2}}-\frac{N_{\mathrm{min}}^{2}}{N_{\mathrm{probe}}^{2}}\right]^{0.5} \tag{5}$$

Because the Doppler burst length L_{D} can be defined geometrically as the number of signal periods above the burst detector trigger level multiplied by the fringe spacing, the minimal Doppler burst length is

$$L_{\mathrm{D}}(d_{\mathrm{min}})=N_{\mathrm{min}}\times\delta \tag{6}$$

And the number of fringes inside the laser probe volume can be denoted as

$$N_{\mathrm{probe}}=\frac{d_{\mathrm{w}}}{(\delta\cos\alpha)} \tag{7}$$

Replacing $L_{\mathrm{D}}(d_{\mathrm{p}i})$ and N_{probe} in Eq. (5) by using Eqs. (6) and (7), respectively, gives the minimal effective diameter of the laser probe volume for the minimal detectable particle diameter

$$D(d_{\mathrm{min}})=0 \tag{8}$$

Because $D(d_{\mathrm{p}i})$ can also be denoted as Eq. (9) according to Sanker et al. [17]:

$$D(d_{\mathrm{p}i})=\left[D^{2}(d_{\mathrm{min}})+d_{\mathrm{w}}^{2}\ln\left(\frac{d_{\mathrm{p}i}}{d_{\mathrm{min}}}\right)\right]^{0.5}$$
$$=d_{\mathrm{w}}\ln^{0.5}\left(\frac{d_{\mathrm{p}i}}{d_{\mathrm{min}}}\right) \tag{9}$$

local transient solid concentration $1-\varepsilon_{\mathrm{tr}}$ can be calculated easily according to Eqs. (3), (4) and (9).

The critical solid concentration for identifying particle clusters is generally denoted as n-times the standard deviation of $1-\varepsilon_{\mathrm{tr}}$ over local time-averaged solid concentration $1-\varepsilon_{\mathrm{t}}$. Many researchers preferred to choose an empirical n through trial-and-error [4,14,18], because n varies with operating conditions to some degree. For example, Soong et al. [14] selected 3.0 for the value of n in their study. A typical

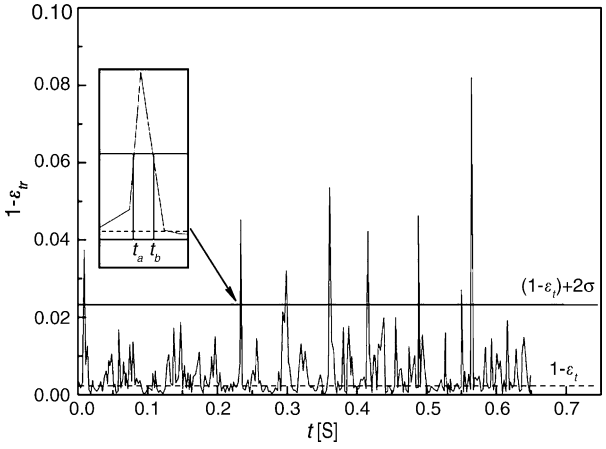

Fig. 3. Time series of local transient solid concentrations.

time series of $1-\varepsilon_{\mathrm{tr}}$ is shown in Fig. 3. Those sharp and distinct spikes (e.g., between t_{a} and t_{b}) over the critical line denoted as $(1-\varepsilon_{\mathrm{t}})+2\sigma$ represent particle clusters existing in the probe volume during the sampling period. It is clear that the number of particle clusters detectable keeps nearly constant when the critical line, the threshold for identifying particle clusters, varies within certain range. If this variation range of n under different operating conditions is found out, an appropriate threshold for identifying particle clusters may be determined easily.

Recognizing this, particle cluster occurrence frequency f_{cl} defined as the number of particle clusters detected per unit time is plotted versus n in Fig. 4. Under different operating conditions, there always exists such a variation range of n within which f_{cl} keeps constant. In order to identify most particle clusters under a given operating condition, it is necessary that the variation range of n should correspond to the range within which the constant f_{cl} first appears when n increases from zero gradually. From Fig. 4, the ranges of n for three cases are $1.6<n<2.1$, $1.8<n<2.2$ and $1.5<n<2.4$, respectively. Their overlap means that f_{cl} remains constant when n varies from $n_{\mathrm{min}}=1.8$ to $n_{\mathrm{max}}=2.1$ under the three operat-

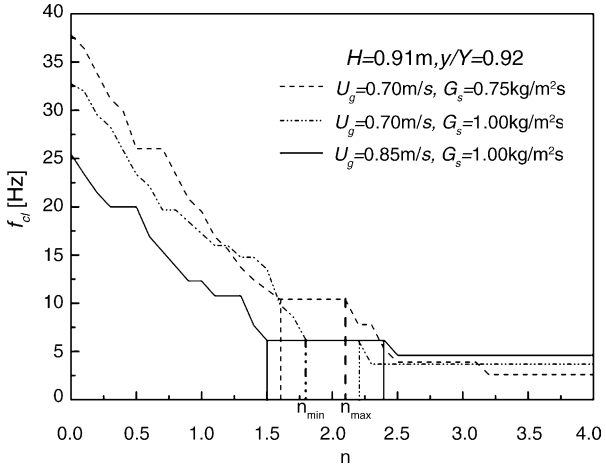

Fig. 4. Variation of occurrence frequency f_{cl} with n.

Table 2
Effects of the value of n on calculated results of particle cluster parameters

	$n = 2.0$	$n = n_{min} = 1.8$		$n = n_{max} = 2.1$	
	Calculated value	Calculated value	Relative error (%)	Calculated value	Relative error (%)
ε_{cl}	0.982	0.983	0.10	0.982	0.00
f_{cl} (Hz)	19.19	21.32	11.10	19.19	0.00
F_{cl} (%)	4.56	5.02	10.09	4.56	0.00
u_{cl} (m/s)	0.016	0.013	−18.75	0.016	0.00

ing conditions. Many discrete particles cannot be rejected if $n < n_{min}$, but some so-called small particle clusters may also not be counted if $n > n_{max}$. So an appropriate n should be chosen between n_{min} and n_{max}.

Inasmuch as n keeps relatively constant when operating parameters keep roughly identical, a semi-empirical method to set n is proposed as follows: (1) to plot f_{cl} as a function of n for some typical operating conditions; (2) to find out the overlap of the first plateau of all the curves in the above figure and to determine corresponding n_{min} and n_{max}; (3) a relatively high n between n_{min} and n_{max} would enable us to identify most particle clusters without interference of background solids. As shown in Table 2, when $n = 2.0$ was chosen at $U_g = 0.70$ m/s, $G_s = 1.00$ kg/m^2 s, $H = 0.91$ m and $y/Y = 0.84$ according to the above steps, relative errors of calculation of particle cluster parameters can be anticipated to be 10% or so in the case of $n_{min} < n < n_{max}$, and even less than 0.10% for voidage inside particle clusters, which indicates that a slight variation of n has little effect on the analysis of particle cluster dynamics in general and $n = 2.0$ is reasonable for us to identify particle clusters in the gas–solid flow under these operating conditions.

In order to improve the accuracy of PDPA measurement in attenuated environments, extra-large particles and velocities outside the chosen range were rejected, and the temporal data files were reconstituted at least three times to exclude measurement errors resulting from Doppler burst splitting [19].

4. Results and discussion

4.1. Hydrodynamic characteristics of the dilute gas–solid flow

The spatial distributions of ε_t, u_p and the standard deviation of particle velocities σ_u were studied primarily by using the PDPA in this subsection since they are closely related to particle cluster properties. Many cross-sectional averaged variables $\langle X_m \rangle$ are obtained by integrating the profiles of local time-averaged variables over the cross-section of the bed as a function of radial dimensionless distance as follows:

$$\langle X_m \rangle = \int_0^1 2 \left(\frac{y}{Y}\right) X_m \left(\frac{y}{Y}\right) d\left(\frac{y}{Y}\right) \quad (10)$$

where $X_m(y/Y)$ denotes a particular property such as local time-averaged voidage, voidage inside particle clusters, occurrence frequency and particle cluster velocities, etc.

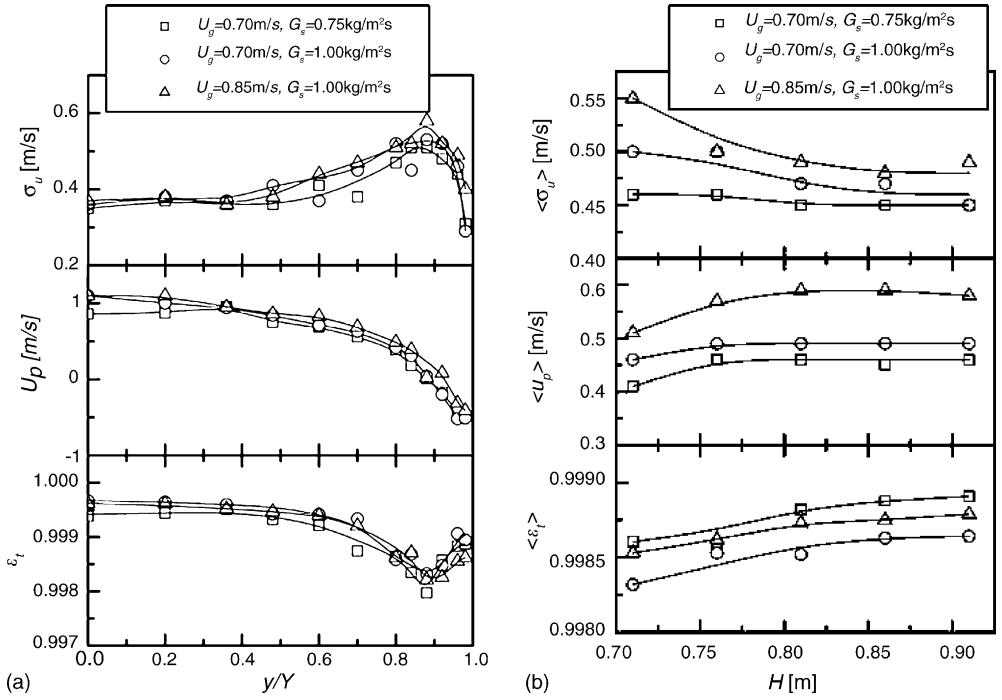

Fig. 5. (a) Radial profiles at $H = 0.81$ m of local time-averaged voidage, particle velocities and particle velocity standard deviation and (b) axial variations of their cross-sectional averaged values under different operating conditions.

It is seen from Fig. 5(a) that the gas–solid flow forms obvious core-annulus structure, but the radial profiles of ε_t for three operating conditions at $H = 0.81$ m differ from those in intermediate or high-density CFB risers, in taking on the shape of a hook and approaching a minimum near the core-annulus boundary. A possible explanation for this special radial distribution might be the accelerated motion of particles in the developing section of the gas–solid flow. Although Wang et al. [20] and Qi [21] also found similar phenomenon, neither did they give any explanation. Particle velocities u_p for three operating conditions decrease obviously towards the bed wall, even changing direction to become negative. And σ_u approaches a maximum near the core-annulus boundary because of the strong interaction between the two regions. Since the extrema of ε_t and σ_u and the zero point of u_p all exist at around $y/Y \approx 0.85$, similar to the findings of Qi et al. [22], this position may be viewed as the core-annulus interface.

Fig. 5(b) shows cross-sectional time-averaged voidage $\langle\varepsilon_t\rangle$ increases with elevation and then approaches constancy in the upper section tested, which quite agrees with the findings of Bai et al. [23]. A higher cross-sectional averaged particle velocity $\langle u_p\rangle$ at a higher elevation indicates the accelerated motion of particles as mentioned above, while the cross-sectional averaged standard deviation of particle velocities $\langle\sigma_u\rangle$ decreases with elevation, as indicated by Van den Moortel et al. [24].

It is worth notice that the axial variations of ε_t and σ_u follow different trends in the core and annulus regions of the fluidized bed, respectively. As shown in Fig. 6, only in the annulus region does ε_t increase with elevation, but keeps relatively constant in the core region. On the contrary, standard deviation of particle velocities σ_u in the core region is much more sensitive to elevation than that in the annulus region, and decreases significantly with elevation in the core region but keeps invariable in the annulus region. While no similar regularity for u_p is perceived under these conditions.

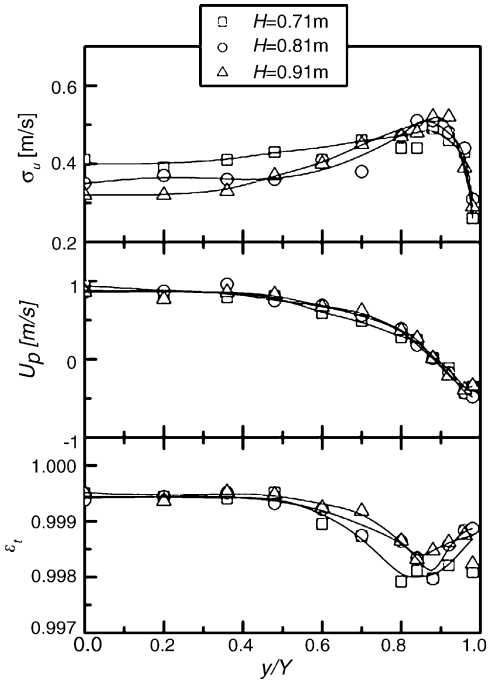

Fig. 6. Radial profiles at $U_g = 0.70$ m/s and $G_s = 0.75$ kg/m^2 s of local time-averaged voidage, particle velocities and particle velocity standard deviation at different elevations.

4.2. Influencing factors of particle cluster properties

Particle cluster properties such as voidage inside particle clusters ε_{cl} and particle cluster velocity u_{cl} are numerical average of the corresponding properties for all detected particle clusters at the same position in a sampling run, as defined respectively as follows:

- The voidage inside an individual particle cluster ε_{cli} is

$$\varepsilon_{cli} = 1 - \sum_{j=1}^{n}\left(\frac{\pi}{6}d_{pj}^3\right) / \sum_{j=1}^{n}[u_{pj}A(d_{pj})(\mathrm{Gt}_j + \mathrm{It}_j)] \quad (11)$$

- Occurrence frequency of particle clusters f_{cl} is defined as the number of particle clusters detected per unit time in a sampling run:

$$f_{cl} = \frac{N_{cl}}{T} \quad (12)$$

- Time fraction of particle clusters F_{cl} is defined as the ratio of the sum of the particle cluster existence time to the total sampling time:

$$F_{cl} = \left(\frac{1}{T}\right)\sum_{i=1}^{N_{cl}}\sum_{j=1}^{n}(\mathrm{Gt}_{ij} + \mathrm{It}_{ij}) \quad (13)$$

- The velocity of an individual particle cluster u_{cli} is given by the local average mass flux on the basis of the mass frame of reference [25]:

$$u_{cli} = \sum_{j=1}^{n}\left[\frac{m_{pj}}{A(d_{pj})}\right] / \sum_{j=1}^{n}\left[\frac{m_{pj}}{u_{pj}A(d_{pj})}\right] \quad (14)$$

This subsection will focus on the effects of ε_t and σ_u on particle cluster properties with respect to the mechanism of particle–particle interaction of particle aggregation.

As shown in Fig. 7(a), voidage inside particle clusters ε_{cl} generally increases with increasing ε_t due to weaker particle–particle interaction. The effects of ε_t on f_{cl} are rather complex: while lower ε_t promotes the aggregation of particles, it also increases particle cluster sizes, which in turn reduces the number of particle clusters [5]. But for dilute gas–solid flow such as in this study, occurrence frequency of particle clusters f_{cl} decreases with increasing ε_t because the decreasing tendency of particle collision frequency resulting from increasing ε_t is the dominant phenomenon. A decreasing F_{cl} with increasing ε_t is reasonable, because an increasing ε_t leads to decreasing f_{cl}, that is, to decreasing the number of

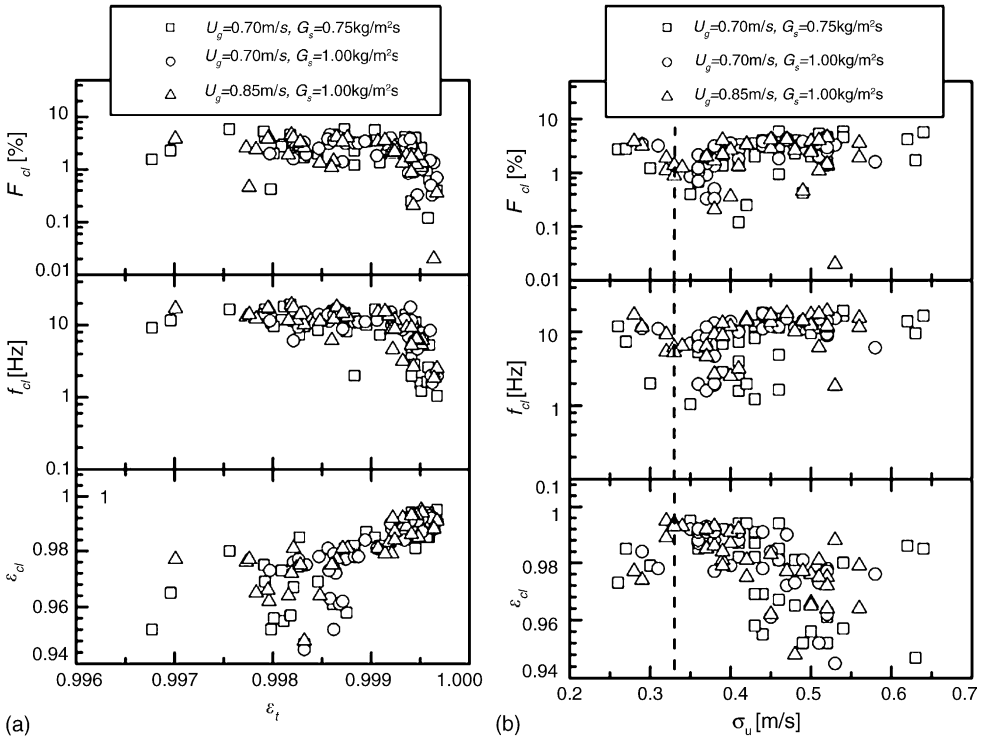

Fig. 7. Variations of particle cluster properties with (a) local time-averaged voidage and (b) particle velocity standard deviation under different operating conditions.

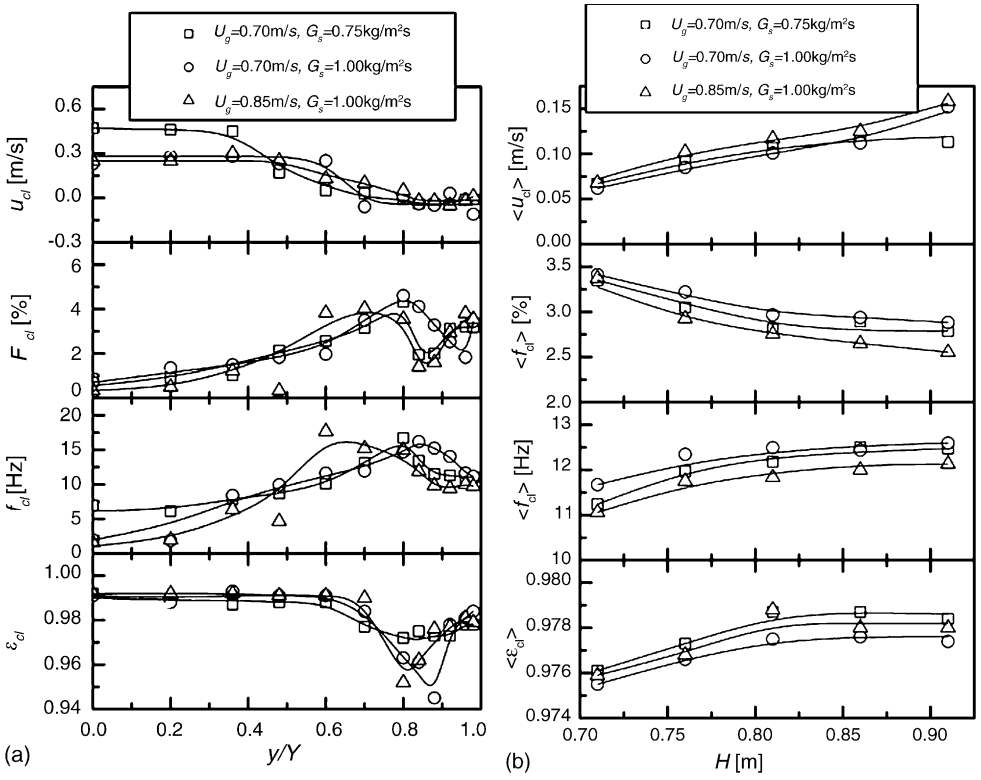

Fig. 8. (a) Radial profiles at H = 0.81 m of particle cluster properties and (b) axial variations of their cross-sectional averaged values under different operating conditions.

particle clusters to pass through the laser probe volume in a sampling run.

It is obvious that an increasing σ_u in the core region means stronger particle–particle interaction there, so a decreasing ε_{cl} occurs when σ_u increases in this region, as shown in Fig. 7(b). But in the adjacent region of the bed wall, where σ_u is generally less than about 0.34 in the experiments (as shown on the left of the dashed line in Fig. 7(b)), an increasing ε_{cl} with increasing σ_u might be because that the aggregation of most particles in this region does not result from the particle–particle interaction but the collision between particles and the wall. Similar to the effects of ε_t on f_{cl}, although an increasing σ_u would lead to increasing the probabilities of both the aggregation of discrete particles and the decomposition of particle clusters in a sense of theory, the former plays a dominant role for such dilute gas–solid flow in this work. So f_{cl} generally increases with increasing σ_u in the core region. But an increase of σ_u at the bed wall must make more particles leave from the wall, and hence lead to decreasing the number density of particle clusters and f_{cl} there. As mentioned above, time fraction of particle clusters F_{cl} is generally dependent upon f_{cl}, so the variation trend of F_{cl} with σ_u is similar to that of f_{cl} in the fluidized bed.

4.3. Radial and axial profiles of particle cluster properties

It can be seen from Fig. 8(a) that ε_{cl} is as high as about 0.99 in the core region, indicating so-called particle clusters in this region are only some very incompact agglomerations of particles. While the measuring point traverses towards the bed wall, voidage inside particle clusters ε_{cl}, similar to the radial profile of ε_t, decreases significantly until reaching a minimum and then increases slightly again near the bed wall, because not only does ε_{cl} decrease with decreasing ε_t and increasing σ_u, but also both the lowest ε_t and the highest σ_u exist near the core-annulus boundary simultaneously (see Fig. 5(a)). The radial profiles of f_{cl} and F_{cl} form peaks near the core-annulus boundary coinciding with those of ε_t and σ_u, because lower ε_t and higher σ_u lead to higher f_{cl} and F_{cl} in this region. Both an increasing ε_t in the wall region and the wall effect may be responsible for the decrease of f_{cl} there. A slight increase in F_{cl} near the bed wall may be partly attributed to increasing particle cluster size resulting from the wall effect. Due to frequent exchange of particles between the core and annulus regions, the radial profiles of u_{cl} under different operating conditions are much more gradual than those of u_p, only forming a step-function decrease near the core-annulus boundary.

Fig. 8(b) shows that cross-sectional averaged voidage inside particle clusters $\langle\varepsilon_{cl}\rangle$ is lower in the lower section and then increases gradually until approaching relative constancy in the upper section, which is also very similar to the axial profile of $\langle\varepsilon_t\rangle$ under the same operating conditions. These strong similarities, although partly resulting from a decreasing σ_u with elevation, also indicate again that ε_{cl} is closely related to ε_t. As a matter of fact, Harris et al. [7] have correlated the averaged solid concentration inside particle clusters in the near wall region with cross-sectional averaged solid concentration in order to predict particle clustering behavior according to macro operating parameters of CFB risers. Compared with the axial variation of $\langle\varepsilon_t\rangle$ (Fig. 5(b)), the same variation of operating parameters leads to much dramatic axial modification of $\langle\varepsilon_{cl}\rangle$. It is believed that particle cluster velocity is dependent upon discrete particle velocities, so cross-sectional averaged velocity of particle clusters $\langle u_{cl}\rangle$, like $\langle u_p\rangle$, also increases with elevation. Because of lower $\langle\sigma_u\rangle$ and higher $\langle\varepsilon_t\rangle$ as well as higher particle cluster velocity on higher elevation, cross-sectional averaged time fraction of particle clusters $\langle F_{cl}\rangle$ decreases with elevation. According to the analysis in former subsection, cross-sectional averaged occurrence frequency of particle clusters $\langle f_{cl}\rangle$ ought to decrease with elevation, but the experimental data in Fig. 8(b) show that the axial variation of $\langle f_{cl}\rangle$ are contrary to this predicting trend because a key influencing factor, the upward accelerated motion of particles, was not taken into account, which has an important effect on $\langle f_{cl}\rangle$ in the developing section of the dilute gas–solid flow. The relevant research on this issue is on-going in our laboratory.

Fig. 9 shows the radial profiles of particle cluster properties at different elevations at $U_g = 0.70$ m/s and $G_s = 0.75$ kg/m^2 s. Combining this figure with Fig. 8(a), it is easy to find that ε_{cl} in the annulus region, varying with U_g, G_s and elevation, is more sensitive to the variation of oper-

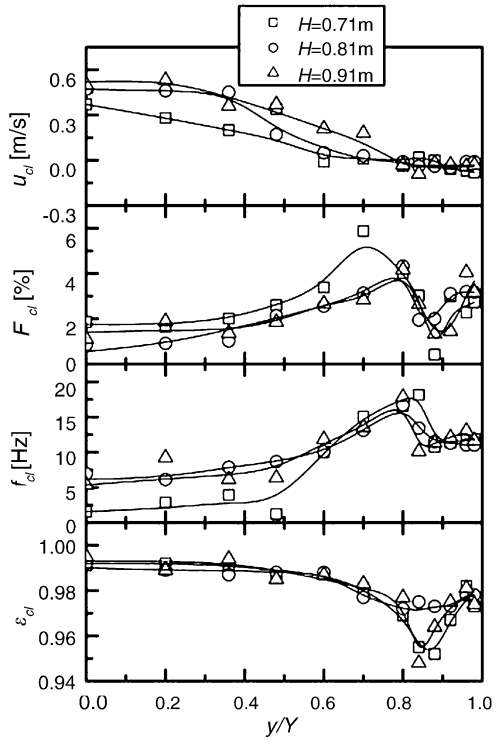

Fig. 9. Radial profiles at $U_g = 0.70$ m/s and $G_s = 0.75$ kg/m^2 s of cluster properties at different elevations.

ating parameters than that in the core region. Particle cluster velocity u_{cl}, differing from u_p, changes with U_g, G_s and elevation in the core region, but has no perceivable modification in the annulus region due to the wall effect. While this regional variation is not obvious for f_{cl} and F_{cl} in the above two figures in this work.

5. Conclusions

Particle cluster properties including voidage inside particle clusters, occurrence frequency, time fraction and particle cluster velocity were investigated in this study by using the PDPA.

- The algorithm proposed in this study provides an effective method for investigating particle clusters in dilute gas–solid suspensions, particularly in exploring the micro and meso structures in dilute particle-fluid two-phase flow.
- The radial profiles of local time-averaged voidage and voidage inside particle clusters in dilute gas–solid fluidized beds differ from those in intermediate or high-density gas–solid fluidized beds.
- The axial and radial distributions of voidage inside particle clusters and particle cluster velocity are similar to those of local time-averaged voidage and discrete particle velocity, respectively.
- It is in the annulus region that voidage inside particle clusters is more sensitive to the variation of operating parameters, but reverse for particle cluster velocity.
- Particle cluster properties, especially voidage inside particle clusters, are closely related to local time-averaged voidage and turbulent fluctuation of particles.

Acknowledgements

The authors would like to express their gratitude to Prof. Mooson Kwauk for his valuable suggestions to this paper. The financial supports from the National Natural Science Foundation of China (90210034, 20221603) and the Research Found for Returned Overseas Chinese Scholars are also gratefully acknowledged.

References

[1] D. Subbarao, P. Basu, A model for heat transfer in circulating fluidized beds, Int. J. Heat Mass Transfer 29 (3) (1986) 487–489.
[2] J. Li, M. Kwauk, Particle-Fluid Two-Phase Flow, the Energy-Minimization Multi-Scale Method, Metallurgical Industry Press, Beijing, 1994.
[3] W.K. Gu, J.C. Chen, A model for solid concentration in circulating fluidized beds, in: L.S. Fan, T.M. Knowlton (Eds.), Fluidization IX, Engineering Foundation, New York, 1998, pp. 501–508.
[4] K. Tuzla, A.K. Sharma, J.C. Chen, T. Schiewe, K.E. Wirth, O. Molerus, Transient dynamics of solid concentration in downer fluidized bed, Powder Technol. 100 (1998) 166–172.
[5] S.V. Manyele, J.H. Parssinen, J.X. Zhu, Characterizing particle aggregates in a high-density and high-flux CFB riser, Chem. Eng. J. 88 (2002) 151–161.
[6] A.K. Sharma, K. Tuzla, J. Matsen, J.C. Chen, Parametric effects of particle size and gas velocity on cluster characteristics in fast fluidized beds, Powder Technol. 111 (2000) 114–122.
[7] A.T. Harris, J.F. Davidson, R.B. Thorpe, The prediction of particle cluster properties in the near wall region of a vertical riser, Powder Technol. 127 (2002) 128–143.
[8] J.R. Grace, J. Tuot, A theory for cluster formation in vertically conveyed suspension of intermediate density, Trans. Inst. Chem. Eng. 57 (1979) 49–54.
[9] J. Li, Y. Tung, M. Kwauk, Method of energy minimization in multi-scale modeling of particle-fluid two-phase flow, in: P. Basu, J.F. Large (Eds.), Circulating Fluidized Bed Technology, vol. II, Pergamon Press, Toronto, 1988, pp. 89–103.
[10] Y. Fujima, K. Tagashira, S. Ohme, S. Ichimura, Y. Arakawa, Conceptual study on fast fluidization formation, in: P. Basu, M. Horio, M. Hasatani (Eds.), Circulating Fluidized Bed Technology, vol. III, Pergamon Press, Toronto, 1991, pp. 85–90.
[11] X. Liu, S. Gao, J. Li, Study on characteristics of particle clusters in gas–solid circulating fluidized beds by using PDPA, J. Chem. Ind. Eng. (Chin.) 55 (4) (2003) 555–562 (in Chinese).
[12] T. Van den Moortel, L. Tadrist, Flow structures in a circulating fluidized bed, in: J.R. Grace, J.X. Zhu, Hugo, de Lasa (Eds.), Proceedings of 7th International Circulating Fluidized Beds Conference, Canadian Society for Chemical Engineering, Ottawa, 2002, pp. 217–224.
[13] P. Cai, S.P. Chen, Y. Jin, Z.Q. Yu, Z.W. Wang, Effect of operating temperature and pressure on the transition from bubbling to turbulent fluidization, AIChE Symp. Ser. 85 (1989) 37–43.
[14] C.H. Soong, K. Tuzla, J.C. Chen, Identification of particle clusters in circulating fluidized bed, in: A.A. Avidan (Ed.), Circulating Fluidized Bed Technology, vol. IV, Pergamon Press, New York, 1993, pp. 615–620.
[15] G. Sun, G. Qian, J. Li, Dynamic measurement of local voidage in dilute regime of a CFB, Eng. Chem. Metal. 17 (3) (1996) 242–247.
[16] M. Saffman, Automatic calibration of LDA measurement volume size, Appl. Optics 26 (13) (1987) 2592–2597.
[17] S.V. Sanker, D.H. Buermann, A.S. Inenaga, K.M. Ibrahim, W.D. Bachalo, Coherent scattering in phase Doppler interferometry: response of frequency domain processors, in: Proceedings of the 7th International Symposium on Application of Laser Techniques to Fluid Mechanics, Lisbon, 1994, pp. 1–8.
[18] A.J. Yan, S.V. Manyele, J.H. Parssinen, J.X. Zhu, The interdependence of micro and macro flow structures under a high-flux flow, in: J.R. Grace, J.X. Zhu, Hugo, de Lasa (Eds.), Proceedings of 7th International Circulating Fluidized Beds Conference, Canadian Society for Chemical Engineering, Ottawa, 2002, pp. 357–364.
[19] T. Van den Moortel, R. Santini, L. Tadrist, J. Pantaloni, Experimental study of the particle flow in a circulating fluidized bed using a phase Doppler particle analyser: a new post-processing data algorithm, Int. J. Multiphase Flow 23 (6) (1997) 1189–1209.
[20] Y. Wang, F. Wei, Z. Wang, Y. Jin, Z. Yu, Radial profiles of solids concentration and velocity in a very fine particle (36 μm) riser, Powder Technol. 96 (1998) 262–266.
[21] X. Qi, Gas–solids two phase flow dynamics in circulating fluidized bed risers, Doctor dissertation, Sichuan University, Chengdu, China, 2003, pp. 171–175.
[22] X. Qi, W. Huang, Y. Pan, J. Zhu, Y. Shi, Study on the solid concentration and the core-annulus structure in a gas–solids CFB riser, J. Sichuan Univ. (Eng. Sci.) 35 (1) (2003) 43–47.

[23] D. Bai, Y. Jin, Z. Yu, J. Zhu, The axial distribution of cross-sectionally averaged voidage in fast fluidized beds, Powder Technol. 71 (1992) 51–58.
[24] T. Van den Moortel, E. Azario, R. Santini, L. Tadrist, Experimental analysis of the gas-particle flow in a circulating fluidized bed using a phase Doppler particle analyzer, Chem. Eng. Sci. 53 (10) (1998) 1883–1899.
[25] R.E. Van de Wall, S.L. Soo, Measurement of particle cloud density and velocity using laser devices, Powder Technol. 81 (1994) 269–278.